

AD-A123 507

UNDERSTANDING DIELECTRIC CURE MONITORING(U)
MASSACHUSETTS INST OF TECH CAMBRIDGE CENTER FOR
MATERIALS SCIENCE AND ENGINEERING S D SENTURIA

1/1

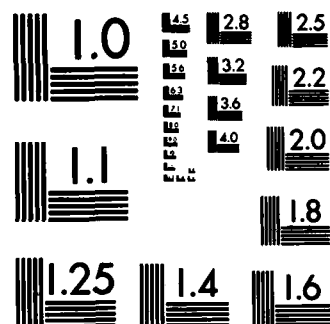
UNCLASSIFIED

05 OCT 82 TR-5 N00014-78-C-0591

F/G 20/3

NL





MICROCOPY RESOLUTION TEST CHART
NATIONAL BUREAU OF STANDARDS-1963-A

(12)

ADA 123507

OFFICE OF NAVAL RESEARCH

Contract N00014-78-C-0591

Task No. NR 356-691

TECHNICAL REPORT NO. 5

UNDERSTANDING DIELECTRIC CURE MONITORING

By

Stephen D. Senturia

Article prepared for publication in

The Adhesion Society Bulletin

MASSACHUSETTS INSTITUTE OF TECHNOLOGY
Department of Electrical Engineering and Computer Science
and Center for Materials Science and Engineering
Cambridge, Massachusetts

October 5, 1982

NOV 13 1982
ELECTE
A

Reproduction in whole or in part is permitted for any purpose
of the United States Government.

This document has been approved for public release and sale;
its distribution is unlimited.

copy

88 01 17 075

UNCLASSIFIED

SECURITY CLASSIFICATION OF THIS PAGE (When Data Entered)

REPORT DOCUMENTATION PAGE		READ INSTRUCTIONS BEFORE COMPLETING FORM
1. REPORT NUMBER	2. GOVT ACCESSION NO.	3. RECIPIENT'S CATALOG NUMBER
	AD-A213 507	
4. TITLE (and Subtitle) Understanding Dielectric Cure Monitoring		5. TYPE OF REPORT & PERIOD COVERED Technical Report 6/82 - 9/82
7. AUTHOR(s) Stephen D. Senturia		6. PERFORMING ORG. REPORT NUMBER Technical Report No. 5
9. PERFORMING ORGANIZATION NAME AND ADDRESS Massachusetts Institute of Technology Department of Electrical Engineering and Computer Science, Cambridge MA 02139		8. CONTRACT OR GRANT NUMBER(s) N00014-78-C-0591
11. CONTROLLING OFFICE NAME AND ADDRESS Department of the Navy, Office of Naval Research 800 N. Quincy Street, Arlington VA 22217 Code 427		10. PROGRAM ELEMENT, PROJECT, TASK AREA & WORK UNIT NUMBERS NR 356-691
14. MONITORING AGENCY NAME & ADDRESS (if different from Controlling Office)		12. REPORT DATE October 5, 1982
		13. NUMBER OF PAGES 7
		15. SECURITY CLASS. (of this report) UNCLASSIFIED
		15a. DECLASSIFICATION/DOWNGRADING SCHEDULE
16. DISTRIBUTION STATEMENT (of this Report) This document has been approved for public release and sale; its distribution is unlimited		
17. DISTRIBUTION STATEMENT (of the abstract entered in Block 20, if different from Report)		
18. SUPPLEMENTARY NOTES		
19. KEY WORDS (Continue on reverse side if necessary and identify by block number) Dielectrometry, cure monitoring, microdielectrometry, conductivity, permittivity, loss factor, resins		
20. ABSTRACT (Continue on reverse side if necessary and identify by block number) An elementary description of the dielectric properties of curing systems, how they are measured, and how they can be interpreted.		

DD FORM 1473

1 JAN 73

EDITION OF 1 NOV 65 IS OBSOLETE
S/N 0102-LF-014-6601

UNCLASSIFIED

SECURITY CLASSIFICATION OF THIS PAGE (When Data Entered)

UNDERSTANDING DIELECTRIC CURE MONITORING

Stephen D. Senturia
Professor of Electrical Engineering
Massachusetts Institute of Technology
Cambridge MA 02139



Introduction

✓ An ideal process monitoring method is one which does not perturb the process, yet somehow provides complete documentation of what is going on. Like all ideals, it is rarely approached in practice, but nevertheless serves to guide the development of suitable methods. The monitoring of the cure of thermosets is a good example. The continuous transition from viscous liquid to rubbery gel to vitreous solid characteristic of thermosets produces such large changes in properties that almost any method of physical measurement can be expected to yield a useful result. In practice, however, techniques such as calorimetry, infrared spectroscopy, and dynamical mechanical measurements, all of which yield highly useful information, tend to be confined to carefully controlled laboratory situations because of the difficulties of in-situ use. For cure monitoring in the manufacturing environment, alternative techniques are needed.

↑ Electrical measurements offer an attractive possibility. During the past decade, various in-situ methods for examining changes in the electrical conductivity of resins during cure have been developed, as have methods for studying changes in dielectric properties. It is useful to group "electrical conductivity" and "dielectric properties" under the common heading "dielectric properties", because, as will be shown below, measurements of the frequency dependence of dielectric properties can yield information both on the conductivity and on the dielectric properties usually associated with hindered dipole rotation.

Parallel Plate Measurements

The most common form of dielectric measurement involves a pair of parallel plates or foils either placed in contact with or embedded into the specimen. The electrode pair form a circuit element which can be represented as a capacitor in parallel with a conductor. The capacitance of the capacitor depends on the area of the plates, the spacing between the plates, and on the dielectric permittivity ϵ' of the medium between the plates. If the permittivity is dispersive (i.e., frequency dependent), then the measured capacitance would also depend on frequency. The conductance of the conductor in parallel with the capacitor depends similarly on the plate area and spacing, and also depends on the conductivity of the medium σ . If σ depends on frequency, then the conductance would also. A conventional way of relating the permittivity and conductivity contributions to one another is to define a quantity with the same dimensions as ϵ' , but proportional to conductivity. From basic

theory, the correct corresponding quantity, called the loss factor and denoted by ϵ'' , and is equal to σ/ω , where ω is the angular frequency at which both ϵ' and ϵ'' are measured. Both ϵ' and ϵ'' are usually reported in units of the permittivity of free space ϵ_0 , which has the value 8.85×10^{-14} Farads/cm. In this case, the ϵ' value corresponds to the conventionally defined dielectric constant, and a material with an ϵ'' value of unity at a frequency of 1 Hz has a conductivity equal to $5.56 \times 10^{-13} \text{ (Ohm cm)}^{-1}$.

Because both the capacitance and conductance measured from parallel plates depend directly on plate spacing, and because this spacing typically changes during a cure cycle either by shrinkage of the curing material or through the application of pressure part-way through the cure cycle, one usually finds reports of the ratio of ϵ'' to ϵ' , called the loss tangent (or, conventionally, $\tan \delta$). Other authors report the dissipation factor D of the capacitor, which is experimentally equivalent to $\tan \delta$. In either case, the reason for reporting $\tan \delta$ or D is that the plate spacing and area both cancel out in the ratio. This has the benefit of yielding a result that is relatively insensitive to geometric changes, but has the disadvantage of preventing simultaneous separate measurements of ϵ' or ϵ'' . When $\tan \delta$ is observed to change, one does not know a priori whether to attribute that change to ϵ' , to ϵ'' , or to both.

Measurements on parallel plate electrodes involve some form of capacitance bridge. Since the measurement apparatus is separated from the plates by cables, the very tiny currents that charge and discharge the cable capacitances coupled with electrostatic noise pickup on the cabling ultimately limit the lowest frequency at which satisfactory measurements can be performed. Typical values of this low-frequency limit are on the order of 100 Hz, although some extensions to lower frequencies are possible with extremely careful design. At the high frequency end, cable inductance eventually limits measurement accuracy, typically in the 100 kHz - 1 Mhz range.

Microdielectrometry

An alternative to the parallel plate approach to dielectric property measurements has recently been developed in our laboratories at MIT. The electrodes form an interdigitated pair, or comb pattern, on the surface of a 2x4 mm integrated circuit (or "chip"). The sample is placed directly on these electrodes; alternatively, the chip is embedded in the material undergoing cure. One of the electrodes is driven with a sinusoidal signal, and field-effect-transistor amplifiers within the chip detect the amount of charge reaching the other electrode through the sample medium. For a given chip geometry, calibration tables which relate the magnitude and relative phase of this charge to the ϵ' and ϵ'' values for the medium have been developed. The electrode geometry does not depend on temperature, pressure, or on shrinkage during cure. Furthermore, given the precision of modern microelectronic fabrication methods, different chips are sufficiently identical to one another so that individual calibration is not required. Because of the built-in amplification, there is no low-frequency limitation to the measurement other than the intrinsic reaction rate of the medium being studied, which represents a significant advantage over parallel

plate methods. A semiconductor diode temperature sensor is also built into the chip, so that extremely local temperature changes during cure can be monitored. The chip is connected through fine wires to electronic instrumentation which, under control of a desktop calculator, sequences the measurement frequency, performs the measurement, interprets the data to yield ϵ' and ϵ'' (and, if desired, temperature), logs the data onto magnetic cassette, and generates real-time display of the data.

Using the Microdielectrometry system, we have studied the cure of a number of thermosetting systems as functions of time, temperature, and frequency. We consistently find that the frequency dependence of both ϵ' and ϵ'' must be examined in order to provide meaningful interpretation of the data. A general model for how ϵ' and ϵ'' change is described below.

Understanding the Data

In our most elementary model, the permittivity is represented as consisting of a constant ϵ_∞ (the equivalent high-frequency dielectric constant) plus a Debye-like dipole orientation term,

$$\epsilon' = \epsilon_\infty + \frac{(\epsilon_s - \epsilon_\infty)}{1 + (\omega\tau)^2}$$

where ϵ_s is the permittivity one measures at low frequency, and τ is the dielectric relaxation time. Note that for $\omega\tau=1$, ϵ' falls at the midpoint between ϵ_s and ϵ_∞ . Corresponding to the dipole term in ϵ' there is a frequency dependent contribution to ϵ'' which exhibits a peak at $\omega\tau=1$. We also add a bulk conductivity term, σ/ω , where in the elementary model, σ is frequency-independent, yielding a total ϵ'' of the form,

$$\epsilon'' = \frac{\sigma}{\omega} + \frac{(\epsilon_s - \epsilon_\infty)\omega\tau}{1 + (\omega\tau)^2}$$

The parameters ϵ_∞ , ϵ_s , and τ characterize the permittivity, and σ plus the other parameters characterize the loss factor. In particular, the frequency dependence of ϵ'' can provide immediate insight into whether one's measurements are dominated by the conductivity term or by the dipole term. An example will be helpful.

If we assume that the bulk conductivity of a curing system falls exponentially with time due to an increase in viscosity produced by crosslinking, and if we also assume that the dipole relaxation time grows exponentially with time for the same reason, then for typical initial values of σ and τ , the "Theory" curves of ϵ' and ϵ'' versus time shown in Figure 1 would be expected. Note the characteristic decrease in ϵ' at successively lower frequencies as τ grows with time (a classic relaxation), and note the corresponding loss peaks in ϵ'' . At 1000 Hz in the example, the loss factor drops, then increases, then drops again during cure. Further, note that early in cure, ϵ'' decreases monotonically with increasing frequency, but when the point is reached where the dipole loss peaks show up, the frequency dependence becomes complex. Since as one approaches the loss peaks, ϵ' is also changing with frequency, if one can only

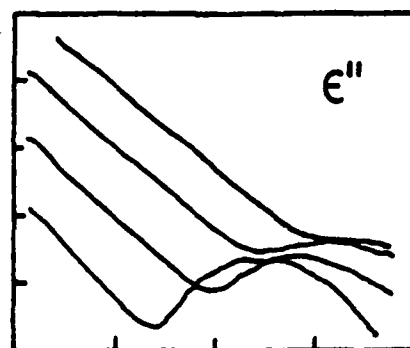
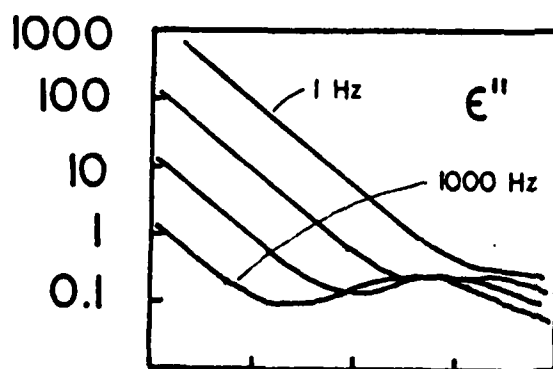
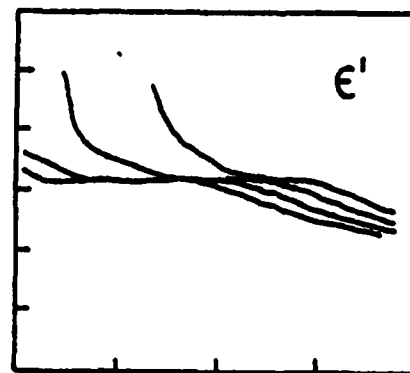
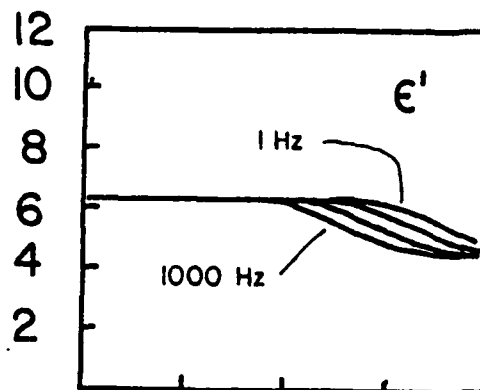
measure the ratio of ϵ'' to ϵ' , one cannot easily assign an origin to observed frequency variation. There is a distinct advantage, therefore, in obtaining separate measurements of both ϵ' and ϵ'' .

To illustrate the reasonableness of the elementary model, the "Experiment" side of Figure 1 shows actual data from an isothermal cure of an amine-epoxy system. The only major differences between the Experiment and the Theory in Figure 1 are the dispersion early in cure in ϵ' , which is attributable to ionic conduction with blocked electrodes, and the persistence of relatively high loss factors at the end of cure, which is attributable to the drop in reaction rate due to vitrification of the sample.

The model outlined above represents a useful starting point for interpreting dielectric data during cure. Rate of change of loss factor can be related to reaction rate. The detailed shape of the dipole orientation peaks can be related to the distribution of relaxation times within the sample, which can, in principle at least, be related to properties of the network being formed by crosslinking. In every case, however, measurements of both ϵ' and ϵ'' over a wide frequency range are required to permit meaningful interpretation of the results.

THEORY

EXPERIMENT



TIME →

TECHNICAL REPORT DISTRIBUTION LIST, GEN

	No. Copies		No. Copies
Office of Naval Research Attn: Code 413 800 North Quincy Street Arlington, VA 22217	(2)	Naval Ocean Systems Center Attn: Mr. Joe McCartney San Diego, CA 92152	(1)
ONR Pasadena Detachment Attn: Dr. R. J. Marcus 1030 East Green Street Pasadena, CA 91106	(1)	Naval Weapons Center Attn: Dr. A. B. Amster, Chemistry Division China Lake, CA 93555	(1)
Commander, Naval Air Systems Command Attn: Code 310C (H. Rosenwasser) Department of the Navy Washington, DC 20360	(1)	Naval Civil Engineering Laboratory Attn: Dr. R. W. Drisko Port Hueneme, CA 93401	(1)
Defense Technical Information Center Building 5, Cameron Station Alexandria, VA 22314	(12)	Dean William Tolles Naval Postgraduate School Monterey, CA 93940	(1)
Dr. Fred Saalfeld Chemistry Division, Code 6100 Naval Research Laboratory Washington, DC 20375	(1)	Mr. John Boyle Materials Branch Naval Ship Engineering Center Philadelphia, PA 19112	(1)
U.S. Army Research Office Attn: CRD-AA-IP P. O. Box 12211 Research Triangle Park, NC 27709	(1)	Scientific Advisor Commandant of the Marine Corps (Code RD-1) Washington, DC 20380	(1)
Mr. Vincent Schaper DTNSRDC Code 2803 Annapolis, MD 21402 Chicago, IL 60605	(1)	Naval Ship Research and Development Center Attn: Dr. G. Bosmajian, Applied Chemistry Division Annapolis, MD 21401	(1)
Naval Ocean Systems Center Attn: Dr. S. Yamamoto, Marine Sciences Division San Diego, CA 91232	(1)	Mr. A. M. Anzalone Administrative Librarian PLASTEC/ARRADCOM Bldg 3401 Dover, NJ 07801	(1)

TECHNICAL REPORT DISTRIBUTION LIST, GEN

	No. Copies		No. Copies
Dr. E. Baer Department of Macromolecular Science Case Western Reserve University Cleveland, OH 44106	(1)	Picatinny Arsenal Attn: A. M. Anzalone, Bldg. 3401 SMUPA-FR-M-D Dover, NJ 07801	(1)
Dr. M. Broadhurst Bulk Properties Section National Bureau of Standards U.S. Department of Commerce Washington, DC 20234	(2)	Dr. J. K. Gillham Department of Chemistry Princeton University Princeton, NJ 08540	(1)
Dr. K. D. Pae Department of Mechanics and Materials Science Rutgers University New Brunswick, NJ 08903	(1)	NASA-Lewis Research Center Attn: Dr. T. T. Serofini, MS-49-1 2100 Brookpark Road Cleveland, OH 44135	(1)
Naval Surface Weapons Center Attn: Dr. J. M. Augl, Dr. B. Hartman White Oak Silver Spring, MD 20910	(1)	Dr. Charles H. Sherman Code TD 121 Naval Underwater Systems Center New London, CT 06320	(1)
Dr. G. Goodman Globe Union Incorporated 5757 North Green Bay Avenue Milwaukee, Wisconsin 53201	(1)	Dr. William Risen Department of Chemistry Brown University Providence, RI 02192	(1)
Prof. Hatsuo Ishida Department of Macromolecular Science Case-Western Reserve University Cleveland, OH 44106	(1)	Dr. J. White Chemical and Metallurgical Engineering University of Tennessee Knoxville, TN 37916	(1)
Dr. John Lundberg School of Textile Engineering Georgia Institute of Technology Atlanta, GA 30332	(1)	Dr. T. J. Reinhart, Jr., Chief Composite and Fibrous Materials Branch Nonmetallic Materials Division Department of the Air Force Air Force Materials Laboratory (AFSC) Wright-Patterson AFB, OH 45433	(1)
Dr. C. Giori IIT Research Institute 10 West 35 Street Chicago, IL 60616	(1)	Dr. J. Lando Department of Macromolecular Science Case Western Reserve University Cleveland, OH 44106	(1)
Dr. R. S. Roe Department of Materials Science and Metallurgical Engineering University of Cincinnati Cincinnati, OH 45221	(1)	Dr. J. A. Manson Materials Research Center Lehigh University Bethlehem, PA 18015	(1)

Dr. Robert E. Cohen (1)
Chemical Engineering Department
Massachusetts Institute of Technology
Cambridge, MA 02139

Dr. T. P. Conlon, Jr., Code 3622 (1)
Sandia Laboratories
Sandia Corporation
Albuquerque, NM

Dr. Martin Kaufman (1)
Code 38506
Naval Weapons Center
China Lake, CA 93555

Prof. C. S. Paik Sung (1)
Department of Materials Science and
Engineering, Room 8-109
Massachusetts Institute of Technology
Cambridge, MA 02139

Dr. Curtis W. Frank (1)
Department of Chemical Engineering
Stanford University
Stanford, CA 94035

Mr. Robert W. Jones
Advanced Projects Manager
Hughes Aircraft Company
Mail Station D 132
Culver City, CA 90230

Dr. R. F. Helmreich (1)
Contract RD E
Dow Chemical Co.
Midland, MI 48640

Dr. R. S. Porter (1)
Department of Polymer Science
and Engineering
University of Massachusetts
Amherst, MA 01002

Prof. Garth Wilkes (1)
Department of Chemical Engineering
Virginia Polytechnic Institute and
State University
Blacksburg, VA 24061

Dr. David Soong (1)
Department of Chemical Engineering
University of California
Berkeley, CA 94720

Prof. Brian Newman (1)
Department of Mechanics and
Materials Science
Rutgers, The State University
Piscataway, NJ 08854

END

FILMED

2-83

DTIC